

**Fig. 5.** A precession photograph ( $\mu = 6^\circ$ ) of the  $hk0$  zone of the reciprocal lattice of the lysozyme protein crystal and its apophyllite substrate seen in Fig. 3. A Buerger precession camera and nickel-filtered  $\text{CuK}\alpha$  x-rays generated by a rotating anode source were used. The x-ray beam was directed to strike both the protein and the mineral crystal so that both reciprocal lattices were recorded simultaneously. The  $h$  and  $k$  reciprocal lattice directions for the lysozyme crystal are indicated on the photograph. Evident from the photograph is the virtual alignment of the reciprocal lattice nets of the two crystals, consistent with the growth of the protein crystal by epitaxy.

al were determined. The rectangular crystals of canavalin induced by magnetite and seen in Fig. 2L were of space group  $C222_1$  ( $a = 136 \text{ \AA}$ ,  $b = 152 \text{ \AA}$ ,  $c = 131 \text{ \AA}$ ) rather than the standard rhombohedral unit cell (4) of  $R3$  symmetry ( $a = 81.3 \text{ \AA}$ ,  $\gamma = 111^\circ$ ) seen in most other experimental trials.

The catalase crystals most frequently observed and consistently so (Fig. 2, A, C, D, E) in the presence of mineral nucleants are of orthorhombic symmetry  $P2_12_12_1$  ( $a = 89 \text{ \AA}$ ,  $b = 140 \text{ \AA}$ ,  $c = 231 \text{ \AA}$ ) (6). The needle crystals seen growing on the mineral gypsum in Fig. 2B, however, were of the trigonal space group  $P3_121$  ( $a = b = 178 \text{ \AA}$ ,  $c = 241 \text{ \AA}$ ), similar to those reported elsewhere (9, 10). Similarly, the standard crystal form of concanavalin B (5) is of hexagonal space group  $P6_3$  ( $a = b = 81 \text{ \AA}$ ,  $c = 101 \text{ \AA}$ ), but in the presence of sandbornite (Fig. 2I) a new form of orthorhombic symmetry  $P2_12_12_1$  was found ( $a = 78 \text{ \AA}$ ,  $b = 62 \text{ \AA}$ ,  $c = 124 \text{ \AA}$ ).

In general, the mineral substrates were quite irregular in form and faces were, in most cases, difficult to identify. Nonetheless, for most samples the growth of the protein crystals from substrates exhibited essentially random orientation and displayed no mutual alignment of crystal faces. This was not, however, true for all. In some samples, it did indeed appear that axial alignment was present between protein crystal and mineral crystal.

The most prominent example of such

apparent alignment was the growth of lysozyme crystals on the mineral apophyllite (Fig. 3). The morphological edges of the mineral and protein crystals are virtually parallel. A calculation of the periodic spacings characterizing the major crystal faces of apophyllite and a comparison with the lattice spacings on the major faces of tetragonal lysozyme crystals (11) demonstrated that a 3 by 5 array of unit cells on the (110) face of apophyllite (12) superimposes on the (100) face of lysozyme with a discrepancy of 0.13 and 0.53%. This is illustrated in Fig. 4. Perhaps more significant, the areal match was within 0.40%. This is extraordinarily good even for the best cases of epitaxial growth of conventional inorganic crystals.

The crystal of lysozyme on the apophyllite substrate seen in Fig. 3 was mounted in a glass capillary by conventional methods (13) and photographed on a Buerger precession camera. With the x-ray beam directed to strike substrate and protein crystal, both the mineral and protein reciprocal lattices could be recorded simultaneously on the same film. One such photograph is shown in Fig. 5. Evident in this diffraction photograph is the virtual alignment of the reciprocal lattices of the substrate and protein crystals. This is convincing evidence for congruence of the crystalline lattices, and it suggests that epitaxial nucleation of protein on the mineral occurred.

The results presented here demonstrate not only that heterogeneous nucleation of proteins on mineral surfaces can occur at lower levels of critical supersaturation, but that epitaxial growth of protein on mineral

crystals can occur. They further suggest that mineral surfaces have organizational properties with respect to biomolecules that might have significance in other regards. Mineral surfaces, for example, by their organizational capabilities, might have served as primitive catalysts of bioreactions or they could play an important role in the assembly of mineralized tissue. It remains to be seen whether protein-mineral epitaxial interfaces have unusual properties of value in processes other than the promotion of crystal nuclei. There is no reason why the promotion of nucleation of protein crystals by these mechanisms should necessarily be limited to mineral substrates. It seems reasonable that other ordered two-dimensional arrays, as obtained from synthetic materials, might serve as well.

#### REFERENCES

1. A. McPherson, *The Preparation and Analysis of Protein Crystals* (Wiley, New York, 1982).
2. J. B. Sumner, *J. Biol. Chem.* **37**, 137 (1919).
3. ——— and S. F. Howell, *ibid.* **113**, 607 (1936).
4. A. McPherson and R. Spencer, *Arch. Biochem. Biophys.* **169**, 650 (1975).
5. A. McPherson, J. Geller, A. Rich, *Biochem. Biophys. Res. Commun.* **57**, 494 (1974).
6. A. McPherson and A. Rich, *Arch. Biochem. Biophys.* **157**, 23 (1973).
7. G. Alderton and H. L. Fevold, *J. Biol. Chem.* **164**, 1 (1946).
8. A. McPherson and P. Shlichta, *J. Cryst. Growth*, in press.
9. M. G. Rossmann and L. W. Labaw, *J. Mol. Biol.* **29**, 315 (1967).
10. W. Longley, *ibid.* **30**, 323 (1967).
11. L. K. Steinrauf, *Acta Crystallogr.* **12**, 77 (1959).
12. J. D. H. Donnay and H. M. Oudik, *Crystal Data Determinations Tables* (Department of Commerce and JCPOS, Washington, DC, ed. 3, 1977), vol. 2.
13. M. V. King, *Acta Crystallogr.* **7**, 601 (1954).

20 August 1987; accepted 2 December 1987

## Enzymatic Oxidation of Cholesterol Aggregates in Supercritical Carbon Dioxide

T. W. RANDOLPH, D. S. CLARK, H. W. BLANCH, J. M. PRAUSNITZ

Fundamental studies of enzyme-solvent interactions can be conducted with supercritical fluids because small changes in pressure or temperature may bring about great changes in the properties of a single solvent near its critical point. Cholesterol oxidase is active in supercritical carbon dioxide and supercritical carbon dioxide-cosolvent mixtures. Variations in solvent power caused by pressure changes or by the addition of dopants affected the rate of enzymatic oxidation of cholesterol by altering the structure of cholesterol aggregates.

**Z**AKS AND KLIBANOV (1) HAVE shown that many enzymes can function catalytically in organic solvents that contain only small amounts of water. Enzymatic catalysis in nonaqueous media may provide information on enzyme-environment interactions (especially for lipophilic enzymes) and may also provide an

escape from kinetic or equilibrium restraints imposed by the use of water as a solvent. For example, nonaqueous solvents offer higher solubilities for lipophilic compounds such as steroids, and they allow certain enzymatic

Department of Chemical Engineering, University of California, Berkeley, CA 94720.

reactions to run "backwards" (for example, a reaction that is hydrolytic in aqueous solution runs as a synthetic reaction).

Supercritical fluids are appealing non-aqueous solvents for enzymatic catalysis (2). Diffusivities in supercritical fluids may be one or two orders of magnitude higher than in liquid solvents and, although densities approach those of liquids, the viscosities of supercritical fluids are intermediate between those of gases and those of liquids. Near the critical point, small changes in temperature or pressure may result in large solubility changes, which make it possible to control reaction rates and to facilitate the downstream separation steps. Finally, rapid precipitation from a supercritical fluid may produce fine crystalline particles, providing an attractive alternative to mechanical comminution (3).

Carbon dioxide (CO<sub>2</sub>) is a particularly attractive supercritical fluid; its critical temperature of 31.1°C is suitable for processing most biochemicals. Proteins are insoluble in supercritical CO<sub>2</sub>, which offers a simple means for separating catalyst from the reaction mixture. In addition, CO<sub>2</sub> is inert, nonflammable, inexpensive, and nontoxic.

Enzymatic conversion of steroids by supercritical fluid processing may be advantageous. Steroids are nearly insoluble in water; for example, room-temperature cholesterol solubility is 4.7 μM (4). However, at 123 bar and 308 K, cholesterol is about 50 times as soluble in CO<sub>2</sub>. Addition of small amounts of cosolvents to CO<sub>2</sub> (for

example, 3.5 mole percent methanol) may increase the solubility five- or tenfold (5).

Cholesterol oxidase (E.C. 1.1.3.6) catalyzes the oxidation of cholesterol by molecular oxygen to 4-cholesten-3-one, a precursor of interest in the pharmaceutical production of androst-1,4-diene-3,17-dione (6). We examined the kinetics of cholesterol oxidation in supercritical CO<sub>2</sub> and supercritical CO<sub>2</sub>-cosolvent mixtures with cholesterol oxidases isolated from *Streptomyces* sp. and from *Gloeocysticum chrysocreas*.

Batch reactions that used lyophilized cholesterol oxidase from *Streptomyces* sp. (7) showed that the enzyme was active in CO<sub>2</sub> at 100 bar and 308 K (8). Conversions near 100% could be obtained within 1 hour with a sufficient concentration of enzyme. However, at lower enzyme concentrations, product formation ceased after about an hour as a result of enzyme inactivation. The loss of enzymatic activity at 308 K in supercritical CO<sub>2</sub> is apparently due not to the supercritical solvent but to thermal inactivation; cholesterol oxidase from *Streptomyces* sp. exhibited a half-life of 45 to 60 minutes in both aqueous solutions and CO<sub>2</sub> at 308 K.

A more stable cholesterol oxidase from *G. chrysocreas* (9) was covalently immobilized with glutaraldehyde to 50-μm nonporous glass beads (10), which were placed in a continuous-flow, packed-bed reactor. A saturated stream of cholesterol in a 9:1 CO<sub>2</sub>:O<sub>2</sub> mixture was pumped through the reactor (11). The residence time was maintained at 13 seconds. Temperature and pres-

sure were controlled at 308 K and 100 bar, respectively. (Data are not available on the critical point of this CO<sub>2</sub>:O<sub>2</sub> mixture, but the conditions used are well above the pressure where critical opalescence was observed.) Production of 4-cholesten-3-one was monitored by on-line, high-pressure ultraviolet (UV) spectroscopy at 242 nm. Additional samples taken downstream of the reactor were also checked by high-performance liquid chromatography and UV spectroscopy for 4-cholesten-3-one concentration and by-product formation. The activity of cholesterol oxidase from *G. chrysocreas* (Fig. 1) is retained for at least 3 days under supercritical conditions.

Cosolvents were added to the CO<sub>2</sub>:O<sub>2</sub> mixture to investigate the effect of increased cholesterol solubility on rates of reaction. The effects of different cosolvents were varied (Fig. 2). Although cholesterol solubility data are not available for mixtures of CO<sub>2</sub> and butanols, data for the addition of methanol, acetone, or ethanol to CO<sub>2</sub> (5) show that the effect cannot be accounted for by solubility data. Methanol caused a larger solubility increase than ethanol but led to a slight decrease in the reaction rate. Conversely, ethanol addition caused a smaller solubility increase but yielded a substantial increase in reaction rate. Addition of higher molecular weight cosolvents (for example, *tert*-butanol or isobutanol), which were expected to cause small solubility increases, yielded reaction rates four times those for cosolvent-free reaction. Possible explanations include a conformational change in the enzyme caused by interaction with the cosolvent or the possibility that the substrate, cholesterol, forms aggregates in solution (12).

Electron paramagnetic resonance (EPR) spectroscopy was used to study the possible effect of cosolvents on the conformation of the enzyme. Cholesterol oxidase from *G. chrysocreas* was spin-labeled (attaching a stable free radical to the enzyme) with 2,2,5,5-tetramethyl-3-pyrroline-1-oxyl-3-carboxylic acid *N*-hydroxysuccinimide ester (13). The derivatized enzyme was examined by EPR spectroscopy in CO<sub>2</sub> and CO<sub>2</sub>-cosolvent mixtures at 308 K and 100 bar (14). No significant change was seen between the EPR spectrum of spin-labeled enzyme at atmospheric conditions and the spectra at 100 bar in pure CO<sub>2</sub>, CO<sub>2</sub>-methanol mixtures, or CO<sub>2</sub>-*tert*-butanol mixtures. Apparently, no gross conformational changes occur in the enzyme upon addition of small amounts of cosolvent to supercritical CO<sub>2</sub> (15).

To study aggregate formation, we conducted EPR spectroscopy experiments with a spin-labeled derivative of cholesterol, 3-

**Fig. 1.** Activity of cholesterol oxidase from *G. chrysocreas* in CO<sub>2</sub> at 308 K and 101.3 bar. Conversions are based on an equilibrium cholesterol solubility of 125 μM [computed from the data of Wong and Johnston (5), using a density of 690 g/liter measured with a Micro-Motion vibrating U-tube densitometer]. Conditions were as follows: 5 cm by 0.3 cm (inside diameter) reactor; flow rate of 0.414 liter/hour; enzyme immobilized on 50-μm glass beads.

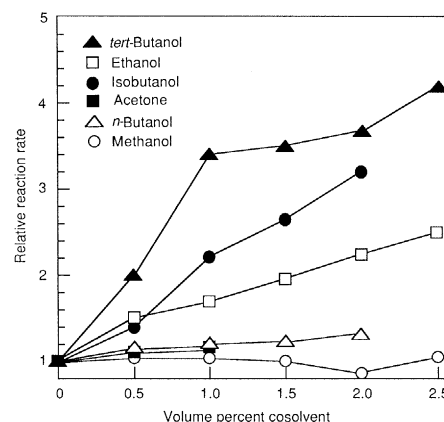
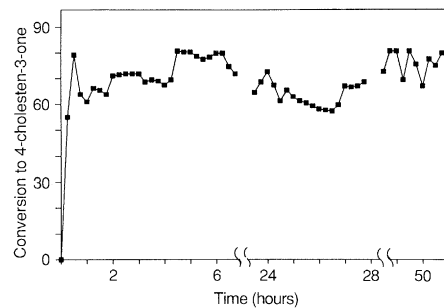


**Fig. 2.** Effect of cosolvent addition on the rate of enzymatic oxidation in supercritical CO<sub>2</sub>. Volume percent cosolvent is based on the unmixed volume of CO<sub>2</sub> and cosolvent.

doxyl-5- $\alpha$  cholestane. In dilute solution (concentrations on the order of  $10^{-3}M$  or less), the EPR spectra of nitroxides undergoing rapid isotropic motion generally appear as three sharp peaks separated by a flat baseline (16). In more concentrated solutions, the three peaks widen as a result of spin-spin interactions between different free radicals, until at sufficiently high concentrations (generally  $>10^{-1}M$ ) the three peaks merge into a single, broad peak. When a  $3.9 \times 10^{-3}M$  solution of 3-doxyl-5- $\alpha$  cholestane in  $CO_2$  at 112 bar and 308 K was examined by EPR spectroscopy, three broad peaks were seen (Fig. 3, curve A). These broad peaks indicated a high local concentration of free radical. Subsequent reduction of spin-labeled cholesterol concentration to  $3.9 \times 10^{-4}M$  and  $6.5 \times 10^{-5}M$  (Fig. 3, curves B and C) did not yield typical low-

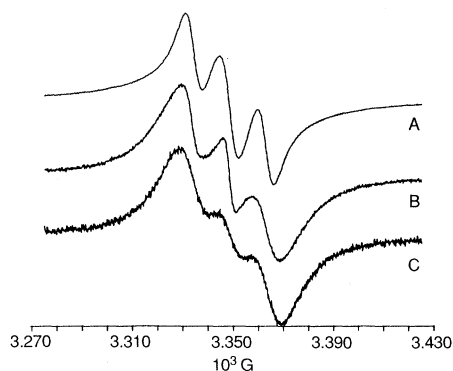


**Fig. 3.** EPR spectra as a function of 3-doxyl-5- $\alpha$  cholestane concentration in supercritical  $CO_2$  at 112 bar and 308 K: curve A,  $3.9 \times 10^{-3}M$ ; curve B,  $3.9 \times 10^{-4}M$ ; curve C,  $6.5 \times 10^{-5}M$ . Relative gains have been adjusted to make all spectra of comparable amplitude.

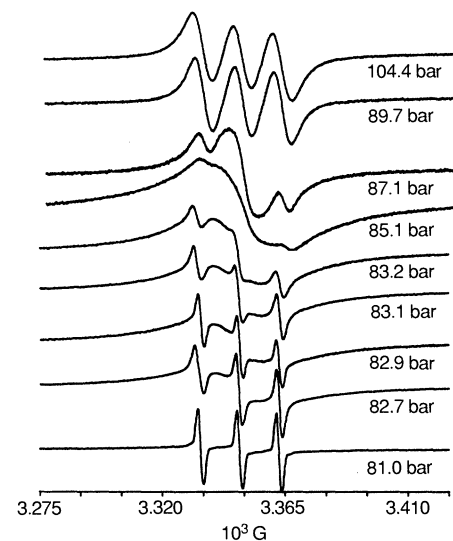


**Fig. 4.** EPR spectra of 0.27 mM 3-doxyl-5- $\alpha$  cholestane with 1.4 mM cholesterol in supercritical  $CO_2$  at 308 K as a function of pressure. Relative gains have been adjusted to make all spectra of comparable amplitude.

concentration spectra; the three peaks remained broad and resembled more closely the single-peak spectrum typical of very concentrated solutions. These observations indicate that the spin-labeled cholesterol formed aggregates, in which the nitroxides were close enough to cause exchange broadening of the EPR signal. Spin broadening was not due to precipitate formation; spectra were always recorded in clear solutions.

As the pressure of a  $CO_2$  solution (1.4 mM cholesterol and 0.27 mM nitroxide-labeled cholesterol) was decreased from 104 to 60 bar, the EPR spectra revealed several regimes (Fig. 4). In the region from approximately 88 to 120 bar, the EPR signal was composed of three broad, sloping peaks that indicate high local free-radical concentration, or aggregation of spin-labeled cholesterol. Between approximately 84 and 88 bar, a transition occurred in the EPR signal. The underlying three-peak signal seen at higher pressures nearly disappeared, leaving only the broad, high local-concentration signal. In this pressure region, the average local concentration of free radicals was greater than that at higher pressures, perhaps as a result of tighter packing of the aggregates.

Liquid micellar systems often exhibit a Krafft temperature below which the surfactant is not soluble enough to allow micelle formation. In a supercritical fluid, we may similarly define a "Krafft pressure," that is, the pressure below which micelles do not form because of limited surfactant solubility. For the cholesterol- $CO_2$  system at 308 K, the Krafft pressure is between 81 and 84 bar, near the critical pressure of  $CO_2$  (73.7 bar). When the pressure is below 84 bar, a sharp, three-peak signal (typical of freely tumbling, monomeric spin label) appears superimposed on the broad aggregate signal. The monomer signal increases in intensity with decreasing pressure, until at 81 bar the aggregate signal has disappeared and all of the spin-labeled cholesterol is present in monomeric form. Below the critical pressure of  $CO_2$ , the spin-labeled cholesterol is no longer solubilized to a sufficient degree for observation by EPR and a flat baseline signal is then observed.

In any study with labeled compounds, it is possible that the label disturbs the phenomenon of interest. When spin-labeled cholesterol was diluted with unlabeled cholesterol (at a constant label concentration of  $8.5 \times 10^{-6}M$ ), substantial peak narrowing occurred. The spectra were asymmetric even when labeled cholesterol was 1% of the total cholesterol. These observations indicate that the local concentration of free radical declines with dilution and that mixed aggregates of labeled and unlabeled cholesterol are formed. Hence, the spin label itself is not

responsible for the aggregation phenomenon.

In liquid micellar systems, cosolvents such as alcohols (especially longer chain alcohols) promote micelle formation (17). Such cosolvents also have a strong effect on the aggregation of spin-labeled cholesterol in supercritical  $CO_2$ . Figure 5 shows the EPR spectra of labeled cholesterol at a constant concentration of  $3.1 \times 10^{-4}M$  in  $CO_2$  at 103 bar and 308 K with 3% (v/v) of various cosolvents added. The bulkier alcohols, *tert*-butanol and isobutanol, have EPR spectra with the highest local concentration of spin label. Addition of methanol and acetone decreases the free-radical packing density. Ethanol promotes a more tightly packed arrangement than *n*-butanol or methanol,

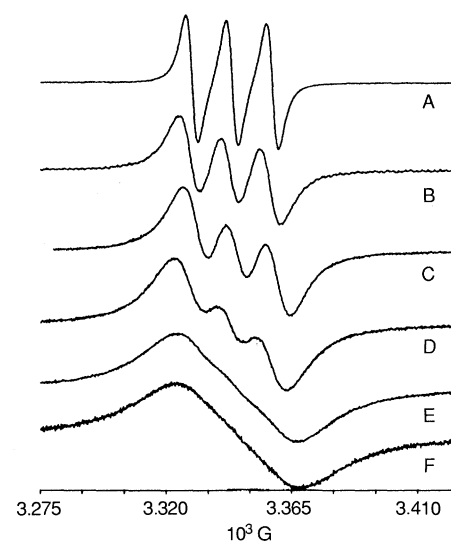


**Fig. 5.** EPR spectra of  $3.1 \times 10^{-4}M$  3-doxyl-5- $\alpha$  cholestane in supercritical  $CO_2$  at 103 bar and 308 K with 3% (v/v) of various cosolvents added: curve A, methanol; curve B, acetone; curve C, *n*-butanol; curve D, ethanol; curve E, *tert*-butanol; curve F, isobutanol.

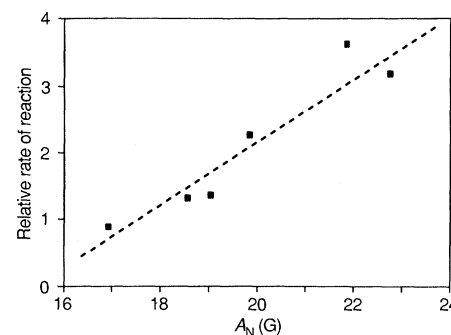


**Fig. 6.** Rate of enzymatic oxidation of cholesterol versus peak splitting in the EPR spectrum of spin-labeled cholesterol in  $CO_2$  at 103 bar and 308 K ( $A_N$  refers to one-half the maximum peak-to-peak splitting in the EPR spectrum). Cosolvent concentration is 2% (v/v) based on premixed volumes. Cosolvents are (in order of increasing peak splitting) methanol, acetone, *n*-butanol, ethanol, *tert*-butanol, and isobutanol.

perhaps because of steric effects. [Ethanol forms solid complexes with cholesterol; methanol does not (5).]

For all of the cosolvents studied, the Krafft pressure was near the critical pressure of CO<sub>2</sub>. Transitions, however, were much less sharp than those observed without cosolvent. A gradual sharpening of the peaks was seen when the pressure fell through the critical region in a solution of spin-labeled cholesterol and 3% (v/v) methanol in CO<sub>2</sub>. The sharpening was more abrupt when *tert*-butanol was the cosolvent. When cosolvents are added to supercritical CO<sub>2</sub>, the broadened Krafft pressure region may be due to increased polydispersity in aggregation number.

There is a good correlation between the degree of spin-spin broadening in the EPR spectrum of spin-labeled cholesterol in various CO<sub>2</sub>-cosolvent mixtures and the observed enhancement in the rate of enzymatic cholesterol oxidation (Fig. 6). The rate of reaction increases when cholesterol is more tightly aggregated and the local concentration of polar hydroxyl groups is higher. EPR spectroscopy indicates that this aggregation is promoted by solvents isobutanol and *tert*-butanol, whereas methanol and acetone do not enhance aggregation. Cholesterol aggregation appears to be the dominant factor affecting the rate of enzymatic oxidation; increased solubility of cholesterol (due to addition of cosolvent to supercritical CO<sub>2</sub>) does not necessarily lead to higher reaction rates.

There are several possible explanations for the enhanced enzymatic activity with the addition of aggregate-enhancing cosolvents such as isobutanol or *tert*-butanol. As with many membrane-bound proteins (18), cholesterol oxidase from *Nocardia rhodocrous* contains a hydrophobic anchor region that confers amphipathic properties on the enzyme, causing the enzyme to bind to hydrophobic membranes and to detergent micelles (19). A detergent micelle or hydrophobic surface is necessary for full enzymatic activity. Although it has not been confirmed that cholesterol oxidase from *G. chrysocreas* has a hydrophobic anchor region, such amphipathic character is likely. Increased hydrophobic surface area due to formation of larger aggregates may allow stronger binding of enzyme to cholesterol aggregates. Cosolvents such as *tert*-butanol and isobutanol may also act as stabilizing "spacers," a well-known phenomenon in liquid micellar systems (20). Increased enzymatic activity may then result from more favorable cholesterol spacing, as occurs in aqueous solution when cholesterol is placed in mixed micelles of dioctanoylphosphatidylcholine (21). Alternatively, increased activity may result

from steering effects caused by the holding of cholesterol molecules in a more rigid orientation than that of monomeric cholesterol free in solution.

#### REFERENCES AND NOTES

1. A. Zaks and A. M. Klibanov, *Proc. Natl. Acad. Sci. U.S.A.* **82**, 3192 (1985).
2. Enzymatic activity in supercritical CO<sub>2</sub> was demonstrated with alkaline phosphatase [T. W. Randolph, H. W. Blanch, J. M. Prausnitz, C. R. Wilke, *Biotechnol. Lett.* **7**, 325 (1985)]. Subsequent investigations have shown that polyphenol oxidase [D. A. Hammond, M. Karel, A. Klibanov, V. J. Krukons, *Appl. Biochem. Biotechnol.* **11**, 393 (1985)] and lipase [K. Nakamura and T. Yano, *Jpn. Kokai Tokyo Koho Patent 61/21098 A2* [86/21098], 29 January 1986] are also active in supercritical CO<sub>2</sub>.
3. K. A. Larson and M. L. King, *Biotechnol. Progr.* **2**, 73 (1986).
4. M. E. Haberland and J. A. Reynolds, *Proc. Natl. Acad. Sci. U.S.A.* **70**, 2313 (1973).
5. J. M. Wong and K. P. Johnston, *Biotechnol. Progr.* **2**, 29 (1986).
6. B. C. Buckland, P. Dunhill, M. D. Lilly, *Biotechnol. Bioeng.* **17**, 815 (1975).
7. From Sigma Chemical, used as received.
8. T. W. Randolph, H. W. Blanch, J. M. Prausnitz, paper presented at the 74th annual meeting of the American Institute of Chemical Engineers, Miami, November 1986.
9. From Chemical Dynamics Corporation. Purity checked by SDS-gel electrophoresis. The protein migrated as one band, with a slight shadow band estimated to compose <2% of the total protein. Used after dialysis against 50 mM phosphate buffer, pH 7.0.
10. From Corning Glass Company. Glass beads were activated and enzyme was immobilized with the method of F. Toldra, N. B. Jansen, and G. T. Tsao [*Biotechnol. Lett.* **8**, 785 (1986)].
11. Reaction rate is zero order in oxygen concentration at these conditions.
12. Local clustering in supercritical fluids has been explored by UV-visible spectroscopy [S. Kim and K. P. Johnston, *Ind. Eng. Chem. Prod. Res. Dev.* **26**, 1206 (1987)].
13. Enzyme (20 mg/ml) was incubated with 100-fold molar excess of 2,2,5,5-tetramethyl-3-pyrrolin-1-oxyl-3-carboxylic acid *N*-hydroxysuccinimide ester (Eastman Kodak, used as received) for 24 hours at room temperature. Excess spin label was removed by dialysis against a 50 mM phosphate buffer, pH 7.0.
14. Labeled enzyme in 50 mM phosphate, pH 7.0, was freeze-dried onto the walls of quartz high-pressure EPR cells. Cosolvents were premixed with CO<sub>2</sub> before addition to the enzyme.
15. Cholesterol oxidase was spin-labeled with a stoichiometry of eight nitroxide groups per enzyme (based on a protein molecular weight of 58,000); a large conformational change would likely be reflected in a change in the EPR spectrum of at least one nitroxide residue.
16. G. I. Likhtenshtein, *Spin Labeling Methods in Molecular Biology* (Wiley, New York, 1976), pp. 40–45.
17. P. L. Luisi and L. J. Magid, *CRC Crit. Rev. Biochem.* **20**, 409 (1986).
18. For example, cytochrome *b<sub>5</sub>* [A. Ito and R. Sato, *J. Biol. Chem.* **243**, 4922 (1968)],  $\gamma$ -glutamyltransferase [R. P. Hugkey and N. P. Curthoys, *ibid.* **251**, 7663 (1976)], or  $\beta$ -lactamase [K. Simons *et al.*, *J. Mol. Biol.* **126**, 673 (1978)].
19. P. S. J. Cheetham, P. Dunhill, M. D. Lilly, *Biochem. J.* **201**, 515 (1982).
20. P. Stenius, in *Reverse Micelles: Biological and Technological Relevance of Amphiphilic Structures in Aqueous Media*, P. L. Luisi and B. E. Straub, Eds. (Plenum, New York, 1984), pp. 1–19.
21. R. A. Burns and M. F. Roberts, *Biochemistry* **20**, 7102 (1981).
22. We thank P. S. Skerker for assistance with the EPR measurements and aid in interpreting EPR spectra and P. Schultz for helpful comments. Supported by the National Science Foundation (grant CBT-8513642) and the Center for Biotechnology Research, San Francisco.

28 August 1987; accepted 7 December 1987

## Cavitation and the Interaction Between Macroscopic Hydrophobic Surfaces

HUGO K. CHRISTENSON AND PER M. CLAESSION\*

The interaction in water of neutral hydrocarbon and fluorocarbon surfaces, prepared by Langmuir-Blodgett deposition of surfactant monolayers, has been investigated. The attraction between these hydrophobic surfaces can be measured at separations of 70 to 90 nanometers and thus is of considerably greater range than previously found. Spontaneous cavitation occurred as soon as the fluorocarbon surfaces were brought into contact but occurred between the hydrocarbon surfaces only after separation from contact. The very long range forces measured are a consequence of the metastability of water films between macroscopic hydrophobic surfaces. Thus the hydrophobic interaction between macroscopic surfaces may not be related to water structure in the same way that the hydrophobic effect between nonpolar molecules is related to water structure.

VERY STRONG LONG-RANGE ATTRACTIVE forces have been measured between macroscopic hydrophobic surfaces in water (1–4). This attraction cannot be accounted for by the classical Derjaguin-Landau-Verwey-Overbeek (DLVO) theory (5, 6) or Lifshitz theory (7, 8), and there has been no satisfactory explanation.

Department of Applied Mathematics, Research School of Physical Sciences, Australian National University, General Post Office Box 4, Canberra, A.C.T. 2601, Australia.

\*Permanent address: Institute for Surface Chemistry, Box 5607, S-114 86, Stockholm, Sweden, and Department of Physical Chemistry, Royal Institute of Technology, S-100 44, Stockholm.